The International Archives of the Photogrammetry, Remote Sensing and Spatial Information Sciences, Volume XLII-2/W7, 2017
ISPRS Geospatial Week 2017, 18–22 September 2017, Wuhan, China

DETECTION OF PERSONS IN MLS POINT CLOUDS USING IMPLICIT SHAPE MODELS

B. Borgmann[a,b]*, M. Hebel[a], M. Arens[a], U. Stilla[b]

[a] Fraunhofer IOSB, Gutleuthausstr. 1, 76275 Ettlingen, Germany
(bjoern.borgmann, marcus.hebel, michael.arens)@iosb.fraunhofer.de
[b] Technical University of Munich, Dept. of Photogrammetry and Remote Sensing, Arcisstr. 21, 80333 Munich, Germany
stilla@tum.de

KEY WORDS: LiDAR, Mobile, Laser scanning, Person, Detection, Classification

ABSTRACT:

In this paper we present an approach for the detection of persons in point clouds gathered by mobile laser scanning (MLS) systems. The approach consists of a preprocessing and the actual detection. The main task of the preprocessing is to reduce the amount of data which has to be processed by the detection. To fulfill this task, the preprocessing consists of ground removal, segmentation and several filters. The detection is based on an implicit shape models (ISM) approach which is an extension to bag-of-words approaches. For this detection method, it is sufficient to work with a small amount of training data. Although in this paper we focus on the detection of persons, our approach is able to detect multiple classes of objects in point clouds. Using a parameterization of the approach which offers a good compromise between detection and runtime performance, we are able to achieve a precision of 0.68 and a recall of 0.76 while having a average runtime of 370 ms per single scan rotation of the rotating head of a typical MLS sensor.

1. INTRODUCTION

The detection of pedestrians (or more general persons) in data which are gathered by mobile laser scanning (MLS) systems is a useful functionality for several use cases. It is, for example, helpful for the save navigation of an autonomous vehicle or the save operation of an autonomous machine in the vicinity of people. It can also be part of a driver assistance system or an assistance system for the operator of a large machine. Such an assistance system could increase the safety of operation if such a machine is used around people. Of course there are also many use cases in the area of human-robot interaction.

Unlike the general detection of obstacles or moving objects, the actual detection of people allows paying particular attention to their safety. An autonomous vehicle can, for example, keep an extra distance to persons or, if a collision could not be avoided, it could be preferable to collide with a wall instead with a person.

There are several challenges to deal with for the detection of persons in use cases like the ones mentioned above. One is that even with modern mobile laser scanning systems the resulting data density of single scans is comparatively low so that often a person is only comprised of 100 - 200 single point measurements. This is demonstrated in Figure 1, which shows a person in different distances in single scans of a LiDAR sensor which is typically used in MLS systems. Another challenge is that many of the use cases depend on real time processing, meaning that the person detection method should be able to process data in the speed of data acquisition. This limits the computational complexity of the method.

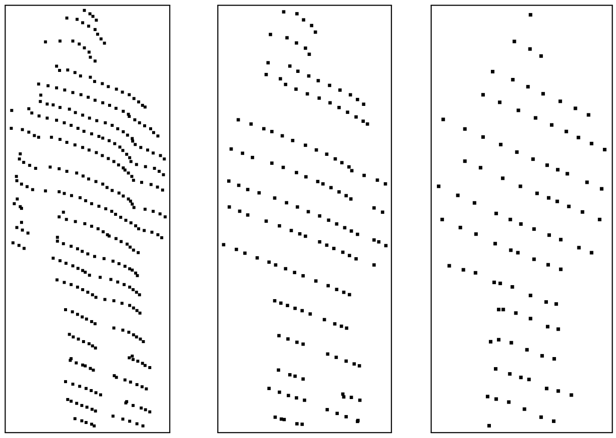

(a) 7.2 m distance (b) 12 m distance (c) 19.5 m distance

Figure 1. Person in a single scan of a Velodyne HDL-64E LiDAR in different distances.

2. RELATED WORK

There are several existing approaches to detect persons or more generally speaking, recognize certain object classes in LiDAR-or other 3D data. One group of such approaches utilize support vector machines (SVM) as a classifier. This classifier is trained by determining a hyperplane in feature space which separates different classes from each other. The hyperplane is then used for the classification of certain data segments. Navarro-Serment et al. (2010) for example present an approach to detect persons in LiDAR point clouds which uses two consecutive SVMs. For the first one, the input are several geometric features, which are created by projecting the data on two different 2-dimensional planes. These planes are created by the first and the second and the first and the third eigenvector of the data. The result of this first SVM is supplemented with several tracking features and used as input for the second SVM, which then generates the actual output of the approach. In another approach, a SVM is used to detect pedestrians in a depth image which is created by combining a LiDAR scan with an RGB image by upsampling the scan into the image (Premebida et al., 2014).

*Corresponding author

Another kind of classifiers are random decision forests. These utilize several decision trees at once and train them with a certain random element. This allows them to deal with the problem of overfitting. Their classification result is generated by merging the results of the different decision trees. They are, for example, used to detect persons and body parts of the persons in depth images generated by Microsoft's KINECT sensor by classifying each pixel of the depth image. They are able to do that in the speed of data acquisition but need depth images with a sufficiently high resolution and a large amount of training datasets (Shotton et al., 2011, 2013).

In recent years, in the field of image-based object recognition a lot of approaches emerged which are based on deep learning and convolutional neural networks (CNNs). These approaches have already been transfered to the area of object recognition in LiDAR-data using either a representation of the data as depth images (Socher et al., 2012) or as volumetric models (Maturana and Scherer, 2015).

Bag-of-words approaches are also widely used to solve classification and recognition problems. These approaches utilize a dictionary with geometrical words. These words are described by a feature descriptor and vote for certain classes. In the classification process, feature descriptors are generated for the processed data and then mapped to words of the dictionary which have a similar descriptor. After that a voting process takes place to classify the data based on the votes of the mapped words. Behley et al. (2013) use several bag-of-words classifiers in parallel which have differently parameterized descriptors. The results of the multiple classifiers are merged later on. The advantage of using multiple bag-of-words classifiers is that they are able to parameterize them to be optimal for different classes and properties of the point cloud segments to classify, like for example different point densities.

Bag-of-words approaches normally do not consider the geometrical distribution and position which the feature descriptors have in the data to classify. There are modifications to the classical bag-of-words method which overcome this disadvantage. One example for that are implicit shape models (ISM) in which each word not only votes for a class but also for a position of the classified object. As part of the voting process, such approaches then look for positions at which votes for a certain class converge to recognize an object. ISM were originally developed to be used on images (Leibe et al., 2008) and were successfully used to detect persons in them (Jüngling and Arens, 2011). Later they were modified to be used on 3D data. Knopp et al. (2010) presented an 3D ISM approach for general object recognition. This approach uses 3D SURF features which are calculated for a set of well picked interest points. Velizhev et al. (2012) also use an ISM approach to detect cars and light poles in 3D point clouds of urban environments. Instead of picking out interest points, they calculate a large amount of the simpler spin images feature descriptor. This descriptor was first presented by Johnson and Hebert (1999). Another ISM approach to detect persons in 3D point clouds is presented by Spinello et al. (2010). In this approach the point clouds are divided into several horizontally stacked layers. Then for each layer segments and features are determined using methods which are normally used for point clouds of 2D LiDAR sensors. After that, the feature descriptors of all layers vote for object positions in the 3D space. Thus, this approach transfers methods for processing 2D LiDAR point clouds to process 3D point clouds.

3. OUR APPROACH

In this section we describe our approach for the detection of persons in 3D LiDAR data. For our approach we assume that the data are provided as general 3D point clouds. This allows us to work also with unstructured point clouds, which result from multiple sensors with different view points. One design criterion of our approach is that it should be able to process the data in the speed of the data acquisition. We also try to work with only a small amount of training data.

A diagram of the approach is shown in Figure 2. It consists of a preprocessing and the actual detection of persons. The preprocessing allows us to reduce the amount of data early on with several lightweight algorithms. This should increase the overall processing speed. The output of the preprocessing are several point cloud segments which could represent a person. These segments are then classified in the classes *person* and *no person* using an ISM approach.

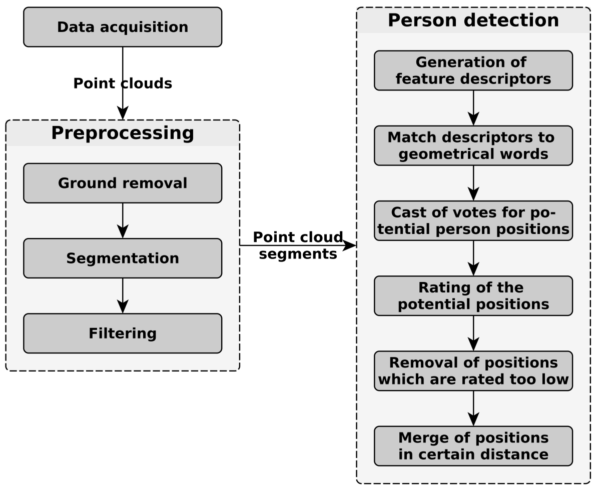

Figure 2. Schematic diagram of our approach

3.1 Preprocessing

The preprocessing is divided into the three consecutive steps: *Removal of ground*, *segmentation* and *filtering of the segments*. Each of these steps is described in this section.

3.1.1 Ground removal The first step of the preprocessing is the removal of the ground. This serves two purposes. It greatly reduces the amount of data and it enables us to properly perform a segmentation in the next step, since otherwise most segments would be connected by the ground. For the ground removal we first generate a ground grid, which describes the surface of the ground. Afterwards we remove every point which is within a certain distance from this grid.

For the generation of the ground grid we assume that we have a height axis in our input data (usually the z-axis). We also assume that the ground is at the bottom of our point cloud. But we are able to deal with a small amount of outliers which are below the actual ground. At first we iterate over the point cloud and group the points in 2-dimensional grid cells according to their coordinates on the x- and y-axis. For each cell we sort the points of that cell according to their coordinate on the height axis and use the value of the 0.05 quantile as height value of the cell. The 0.05 quantile is used to deal with outliers inside that cell.

After we have determined a height value for each cell, we have to evaluate which cells actually contain any ground, since there are cells which contain no ground at all. To do that we recursively traverse the grid originating from a start cell. While traversing, it is checked for the current cell which of its neighboring cells could be reached. A cell counts as reachable if the height difference between it and the current cell does not violate a parameter for the maximum steepness of the ground. Every reachable cell will be traversed and used as a current cell later on, until there are no (not already traversed) reachable cells left. Cells which could not be reached while traversing are removed from the ground grid since we assume that they do not contain any ground. For determining the start cell three criteria are used:

1. The height value of the cell should be between the 0.05 and 0.15 quantile of the height values of all cells. This is done to make sure that the start cell contains ground and to deal with potential outlier cells which have a height value below the actual ground.

2. The number of reachable neighboring cells. Cells with a high amount of reachable neighbors are preferred as start cell.

3. The distance to the center of the grid. Cells near the center are preferred.

3.1.2 Segmentation and filtering As soon as the ground is removed, we perform a region growing segmentation based on the Euclidean distance. After this step points which are part of the same object should be part of the same segment. The segments are then filtered based on several criteria which can be determined with low computational cost. The purpose of this is to reduce the amount of segments which have to be processed by the computationally more expensive detection process.

The first filter which is applied removes segments with only a small amount of points since such segments do not contain enough information to be successfully classified. The second filter uses the geometrical aspect ratio of the segments to remove segments which are basically long lines. For such segments we can say that they are no person. A third filter removes segments which are either too small or too large to be a person.

3.2 Person detection

For the detection of persons in the resulting segments of the preprocessing we use an ISM approach. Such an approach allows us to work with small amounts of training data (Velizhev et al., 2012). In our opinion it has also great potential in dealing with a low point density and is able to process data fast enough to keep up with the data acquisition speed of a MLS system. These are the challenges which we have mentioned in Section 1.

In this section we first give an overview of our approach and its processing steps while detecting objects in the data. Then we will cover several aspects of the approach in greater detail. Although we currently only detect persons, the approach itself is able to detect various kinds of object classes. The processing steps of our approach are:

1. Generation of a feature descriptor for each point of each segment.

2. Search for the best matching geometrical word in the dictionary for each descriptor. For this we use a search index for approximate nearest neighbor searches which is based on the approach presented by Muja and Lowe (2009).

3. Each word of the previous step casts one or more votes for the position of an object of a specific class. This is shown in Figure 3a in a simplified way. Actually every point would have a matching word and cast votes.

4. Rating of the potential object positions for which there are votes. Each vote has a weight in the dictionary. In this step the weight of every potential object position is determined by taking into account the weight of the vote which has voted for the position itself and the weight of votes which have voted for positions for the same object class in the vicinity of the potential position. This step is illustrated in Figure 3b. The size of the dots represents their rating.

5. Removal of all potential object positions which have a weight below a certain threshold (Figure 3c).

6. Merge of the remaining potential object positions for the same class which are in a certain distance from each other (Figure 3d). This acts as a non-maxima suppression and is done by using a region-growing-like method for the potential positions.

7. Output of the resulting object positions as recognized objects.

3.2.1 Feature descriptor The feature descriptor is used to describe local parts of the segments which should be classified and the geometric words in the dictionary. As mentioned in Section 2, there are different strategies for the computing of feature descriptors in ISM approaches. One is to use fewer but more descriptive descriptors which are computed for well picked interest points (Knopp et al., 2010). Another one is to use a less descriptive but faster to compute descriptor and compute it either for a large amount of randomly picked points or for all points of the processed segment (Velizhev et al., 2012). We have decided to use the second strategy since it can deal better with noise and occlusions (Velizhev et al., 2012) which are quite common in point clouds generated by single MLS scans. Hence we use a spin image descriptor (Johnson and Hebert, 1999) which we compute for every point of the segments.

3.2.2 Training and structure of the dictionary The training process uses segments that are already classified to generate the dictionary of geometric words which is later used by the detector. Each geometric word consists of a feature descriptor and at least one vote. On the other hand a vote consists of the class for which the vote is a 3D vector to the voted object position and a weight factor which is between 0 and 1.

In the training process a descriptor is computed for each point in each training segment. After that, this descriptor together with a vector from the point to the position (center) of the training segment and the class information of the segment are used to initialize a new geometric word with one vote for the class and position. The weight of this vote is initialized with 1.

After all training segments have been processed, a k-means clustering of the generated words is performed in the feature space of their descriptors. This clustering puts together words with similar descriptors and is used to merge such words which will then have

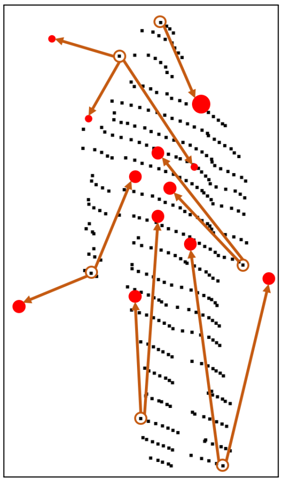

(a) Geometric words have casted votes

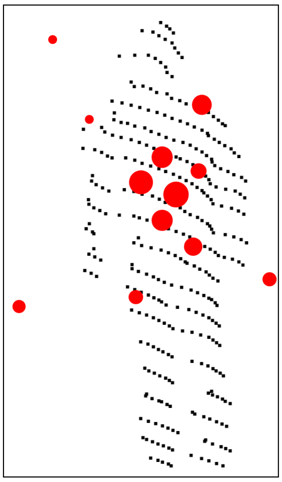

(b) Potential positions are rated

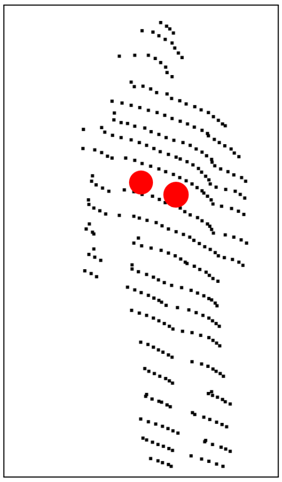

(c) Threshold is applied

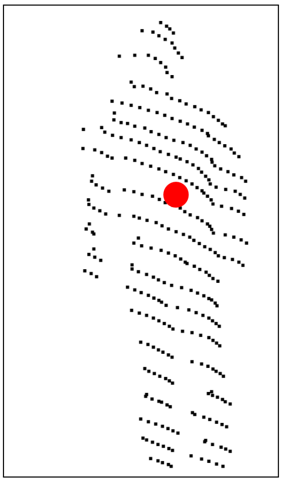

(d) Remaining potential positions in a certain radius merged

Figure 3. Illustration of the main processing step of our person detection

their average descriptor as the descriptor of the merged word. By changing the k parameter of the k-means clustering it is possible to control the size of the resulting dictionary.

After merging, the words will have more than one vote since they inherit all the votes of the original words. These votes are now clustered and merged according to their position vector. This is performed separately for each class for which there are votes. For the clustering of the votes, we use a bottom-up complete linkage hierarchical clustering which we abort if the distance for the next best merge is higher than a threshold. The position vector of the newly merged votes is the average position vector of their original votes. In a final step we recalculate the vote weight for each vote of the merged words:

$$W_v(w_i) = \frac{1}{N_v(w_i)} \tag{1}$$

where $W_v(w_i)$ = Weight for each vote of word w_i
$N_v(w_i)$ = Number of votes of word w_i

This ensures that the total vote weight of each word is 1. This means that votes of words which only cast one or a few votes have a higher weight than votes of words which cast many different votes. Thereby we favor more descriptive words over less descriptive ones.

For the resulting dictionary a search index in the feature space is generated which is later used to find the matching words for feature descriptors. For this search index the approach presented by Muja and Lowe (2009) is utilized. This method allows fast approximate nearest neighbor searches in high-dimensional spaces. It automatically decides between a algorithm based on randomized kd-trees and one based on hierarchical k-means trees and parameterizes them given a desired precision and weight factors for memory usage and index build time.

3.2.3 Rating of potential object positions As already mentioned in Section 3.2, the rating of the potential object positions is step four of our detection process and takes place after each geometrical word, matched with the segment which is currently been processed, has cast its votes. It serves the purpose of determining which of the potential object positions is the position of an actual object. For this we use the soft voting scheme: It is assumed that a high vote weight lays either at or in the vicinity of an actual object position. At the beginning of this step each potential position has the weight of the vote, which originally voted for it (Figure 3a).

At first we determine a normalization factor to limit the total weight of all potential positions to 1:

$$W_{\text{norm}} = \frac{1}{\sum\limits_{p \in P} W_p} \tag{2}$$

where W_{norm} = Normalization factor
W_p = Weight of position p
P = All potential object positions

Afterwards the weight of each potential position is recalculated by taking into account its original weight, the normalization factor and a fraction of the weight of other potential positions for the same class in its vicinity (Figure 3b). This fraction is influenced by the distance between the two positions using the Gaussian normal distribution. So the new weight is calculated as follows:

$$R_p = \sum_{k \in K} W_k \cdot W_{\text{norm}} \cdot e^{-\frac{{D_{pk}}^2}{2\sigma^2}} \tag{3}$$

where R_p = Rated weight of position p
K = All potential positions with same class as p
W_k = Weight of position k
W_{norm} = Normalization factor as defined in (2)
D_{pk} = Euclidean distance between positions p and k
σ = Determines the width of the normal distribution

By changing the factor σ we are able to control how fast the influence of neighboring positions will decrease while the distance increases. To increase the processing speed we ignore positions with a distance greater than 2σ in the actual implementation of the approach.

4. EXPERIMENTS

This section describes several experiments which we have performed to determine the performance of our approach. The experiments cover the influence which the main parameters of the approach have on the runtime and the detection performance. The influence of the used feature descriptor type and its parameters is not examined but we plan to do a comprehensive analysis on that in a future work. At first we will explain our experimental setup and then present and discuss our results.

4.1 Experimental setup

For our experiments we used data which we have acquired with the measurement vehicle "MODISSA"[1]. This vehicle is shown in Figure 4. It is equipped with several LiDAR sensors of which we used the two Velodyne HDL-64E mounted on the roof in the front of the vehicle. These sensors are capable of performing 1.3 million measurements per second in a range up to 120 meters. Their vertical field of view is $26.9°$ which is divided into 64 scan lines. Since they have a rotating head, their horizontal field of view is $360°$. In our setup they rotated with 10 Hz and we considered every rotation as a single scan respectively *point cloud*. This means every point cloud consists of approximately 130.000 measurements. Since not every measurement is successful, for example if it is in the direction of the sky, the resulting point clouds are usually smaller. The vehicle is also equipped with an inertial measurement unit (IMU) and two GNSS receivers. These are used to compensate for the movement of the vehicle while acquiring data which prevents distortion effects.

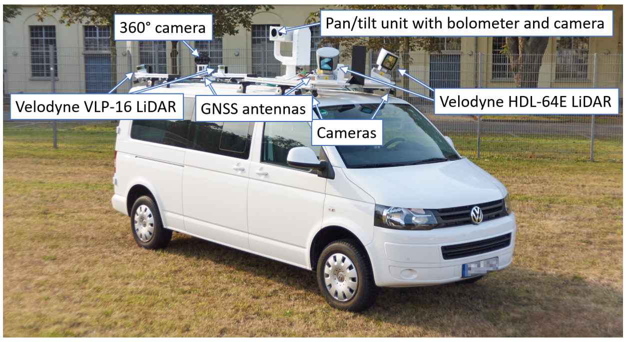

Figure 4. Measurement vehicle MODISSA. Equipped with several sensors including four LiDAR

For the experiments we used two different datasets. One is taken on and around the site of the Technical University of Munich in an urban environment[2]. The second one contains a staged scene with a single person. We used the second dataset mainly for training purposes but parts of that dataset were also used in our evaluation. In total we used 100 point clouds for the evaluation, which were part of multiple short sequences in both datasets. In each of these point clouds persons were annotated manually to create our ground truth. We distinguish between persons which are fully visible in the point clouds and persons which are only partly visible, for example due to occlusions. For the determination of false negative detections we have ignored persons which are only partly visible since it is difficult to decide at which point it should be possible to detect them. Further point clouds were annotated to create a dataset to train our detector. The training dataset contains 244 segments which are a person and 387 examples of segments which are not a person. So our training dataset was comparatively small.

To annotate point clouds for the ground truth and the training data we have processed them with our preprocessing (Section 3.1) and then manually classified the segments. Although this method allows us to annotate point clouds fast and easy, it prohibits us from evaluating the quality of the preprocessing itself. For this we plan to do another analysis in the future.

To evaluate the detection performance of our approach we use the indicators *precision* and *recall* which are defined as follows:

$$Precision = \frac{tp}{tp + fp} \tag{4}$$

$$Recall = \frac{tp}{tp + fn} \tag{5}$$

where tp = True positive detections
fp = False positive detections
fn = False negative detections

The experiments were conducted on a computer with an Intel Core i7-6900k CPU which has 8 cores and can process 16 threads parallel due to hyper-threading. The computer has 64 GB memory which is far more than needed. The implementation of our approach uses parallel processing and is therefore able to profit from the multiple parallel threads of the CPU.

4.2 Results and discussion

This section covers the results of the evaluation of several aspects of our approach.

4.2.1 Preprocessing As already mentioned earlier, due to the method we have used to generate our ground truth data we are not able to evaluate our preprocessing quality-wise. But we have analyzed to which extend it fulfills its main purpose of reducing the amount of data to process later on. For this we have analyzed the amount of points which remain after each step of the preprocessing. The results are listed in Table 1. It shows that on average only 2.25 % of the original point clouds remain after the preprocessing. This is also shown by the example in Figure 5.

	Avg. num. of pts.	Percentage
Unprocessed data	97881	100.00 %
Ground removal	53465	54.62 %
Number of points filter	41730	42.63 %
Aspect ratio filter	34412	35.16 %
Size filter	2203	2.25 %

Table 1. Data reduction in preprocessing

4.2.2 Size of the dictionary The size of the dictionary is one of the main influence factors of our approach. As explained in Section 3.2.2, we can control it by changing the value of k in the k-means clustering. Our training dataset resulted in 263832 geometric words if we do not perform any clustering at all.

At first we evaluated which influence the dictionary size has on the runtime of our approach by comparing the time which is

[1]https://www.iosb.fraunhofer.de/servlet/is/42840/
[2]Data of this measurement campaign can be found at http://s.fhg.de/mls1

https://doi.org/10.5194/isprs-archives-XLII-2-W7-203-2017 | © Authors 2017. CC BY 4.0 License.

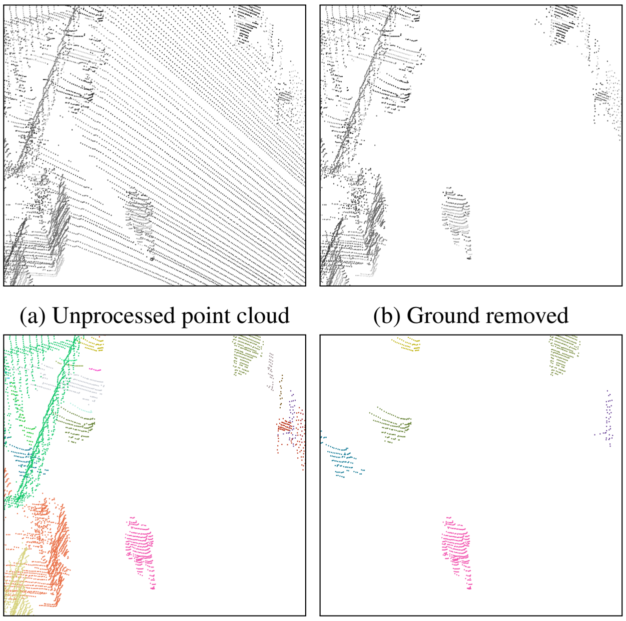

(a) Unprocessed point cloud (b) Ground removed

(c) Segmentation result. Segments are color coded (d) Result of filtering

Figure 5. Processing steps of the preprocessing

needed on average to completely process a single point cloud (preprocessing and detection). This analysis is done by processing the evaluation data with dictionaries in different sizes, but the same other parameters. The result of this analysis is shown in Figure 6.

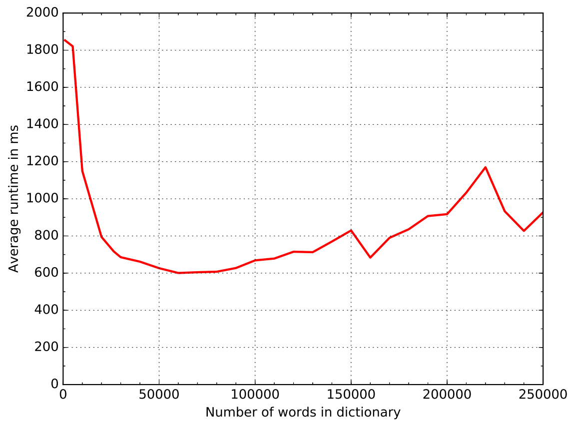

Figure 6. Influence of the dictionary size on the runtime

The size of the dictionary influences the runtime in two ways: On the one hand, it becomes more difficult to find the matching word for the feature descriptor of a point if the dictionary becomes more comprehensive. This is the reason why the runtime, on average, slowly increases with a larger dictionary. On the other hand, merging more words together means that a single word on average casts more votes. This is somewhat compensated since we also merge together similar votes of the same word (Section 3.2.2) but is still a factor. It explains why the average runtime becomes very high when the dictionary is too small for the amount of votes, which is visible on the left of Figure 6.

Figure 7 shows the influence of different dictionary sizes on the precision and recall of our approach. It is shown that there is a slightly better detection performance if the size of the dictionary increases. Therefore we have a trade-off between the runtime and the detection performance of our approach.

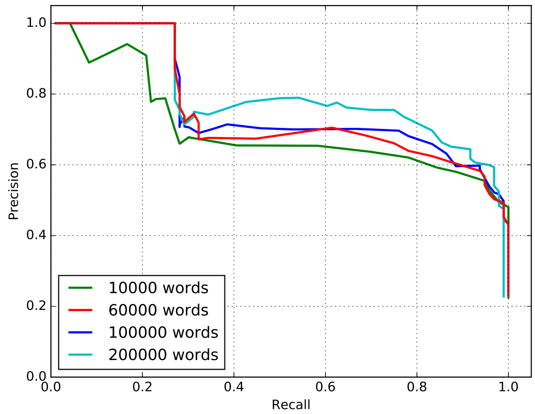

Figure 7. Precision-Recall curve for different dictionary sizes

4.2.3 Rating of potential object positions

As mentioned in Section 3.2.3 the rating of the potential object positions is another crucial step in our detection process. It is influenced by the value of the parameter σ in the formula which is used to calculate the rated weight of the potential object positions (cf. Equation 3).

To analyze the influence of the σ parameter we have done a similar runtime analysis like with the influence of the dictionary size. For this analysis we have used a dictionary with 60000 geometric words, different values for σ and, otherwise, the same parameters. As shown in Figure 8, increasing σ also increases the runtime of the approach. This is to be expected since we consider other potential positions up to a distance of 2σ while rating a single position. Therefore increasing σ means that we have to consider more positions and have to do more calculations for the rating of a single position. At very high values for σ the curve flattened since we reach a point at which we often consider nearly all potential positions of the currently processed segment. In that cases increasing σ further does not increase the complexity of the rating process anymore.

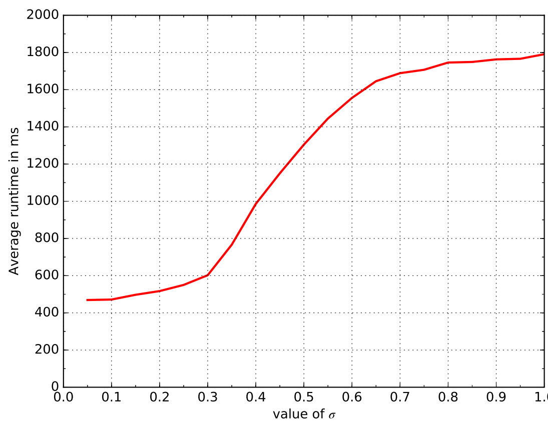

Figure 8. Influence of the value of σ on the runtime

This contribution has been peer-reviewed.
https://doi.org/10.5194/isprs-archives-XLII-2-W7-203-2017

The influence which the parameter σ has on precision and recall of the approach is shown in Figure 9. As with the dictionary size the results show that there is a trade-off between the runtime and the detection performance. It is also shown that a too small σ greatly decreases the detection performance by only slightly increasing the runtime performance. Therefore too small σ-values are not viable.

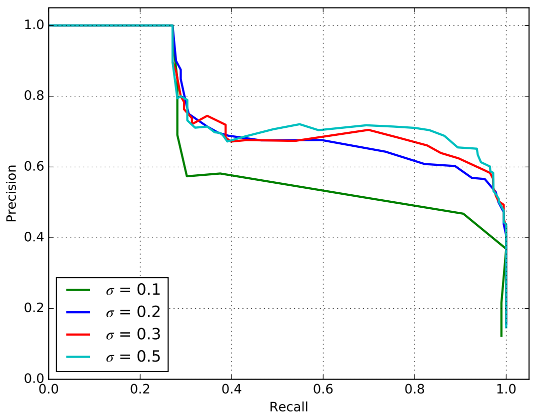

Figure 9. Precision-Recall curve for different values for σ

4.2.4 Further analysis of the runtime Right now we are not completely satisfied with the runtime of our approach. As mentioned earlier we like to be able to process data with approximately the speed of acquisition. Therefore we have analyzed our current approach further to find out which of its components consume how much time. For this we have processed our evaluation data with a dictionary of 60000 words, a σ of 0.3 for the rating of potential positions. These values are a reasonable compromise between the runtime and the detection performance. For this experiment we used 0.17 as threshold for a detection. This parameterization achieves a precision of 0.68 and a recall of 0.76. As before we determined the average runtime per point cloud but this time we break down the runtime for the individual processing steps of the preprocessing and the object detection. The results are shown in Table 2.

	Avg. runtime	**Percentage**
Ground removal	55.12 ms	9.29 %
Segmentation	84.35 ms	14.21 %
Filtering	1.42 ms	0.24 %
Miscellaneous	5.81 ms	0.98 %
Preprocessing	**146.70 ms**	**24.72 %**
Compute features	21.14 ms	3.56 %
Find words and cast votes	252.85 ms	42.60 %
Rate positions	144.41 ms	24.33 %
Miscellaneous	28.44 ms	4.79 %
Object detection	**446.84 ms**	**75.28 %**
Total	**593.54 ms**	

Table 2. Average runtime of each processing step for dictionary of 60000 words and σ of 0.3.

The analysis shows that the search in the dictionary is the most time consuming processing step in our approach. The time needed for this step is determined by the parametrization of the search index and the size of the dictionary as well as the complexity of the feature descriptor. As mentioned earlier we use the approach presented by Muja and Lowe (2009) as search index for the dictionary. Until this point we used 0.95 as precision parameter of that approach. This means that approximately 95 % of the searches for the best matching word would result in the actual best matching word. The build time and memory weight we used is 0 since memory usage is currently no concern of us and we only build the index once as part of our training. Reducing the precision of the search index would be a way to increase the runtime performance of the searches in the dictionary. We performed an experiment to analyze the impact which a reduced search index precision has on the runtime and the detection performance of our approach. For this we repeated the runtime experiment with different search index precisions and otherwise the same parameters. The result of this experiment is visible in Figure 10. It is shown that decreasing the precision of the search index greatly reduces the runtime of searches in the dictionary. Until a certain point the influence on the detection performance is minimal. Using a search index precision of 0.5 reduces the average runtime of the dictionary searches to 32 ms. The total average runtime in that configuration is approximately 370 ms and the achieved precision and recall still are approximately 0.68 and 0.76.

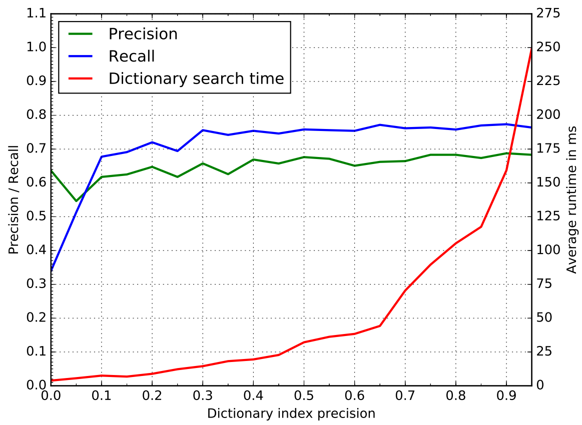

Figure 10. Different desired precisions for the search index of our dictionary and their influence on the detection performance and the runtime of searches in the dictionary

Since we already have used a nearly optimal dictionary size for the given parameters, the remaining potential for runtime improvements of the dictionary searches lies in the feature descriptor. As mentioned earlier the feature descriptor, so far, was not in the focus of our experiments. Currently we use spin images with 153 bins which therefore are represented by 153 dimensional histograms. We think that it is possible to increase the runtime performance of the search in the dictionary if we reduce the dimensionality of the feature descriptor. Whether that is true and how it will affect the detection performance of our approach remains to be analyzed in future experiments. Of course the overall search time could also be decreased by reducing the amount of feature descriptors which are computed.

The rating of the potential object positions is also a time consuming step. As analyzed in Section 4.2.3 it could be improved by reducing the value of the parameter σ but this will have a negative impact on the detection performance. Another way to decrease the runtime of this processing step is to reduce the amount of votes casted. To achieve this either less words have to cast votes or each word has to cast less votes. The first one could be achieved by computing feature descriptors for a smaller amount of points. The second one could be achieved by modifying the threshold for the clustering of similar votes of the same word (Section 3.2.2). But the dictionary which we used for this experiment has 163194 votes and 60000 words. Therefore on average each word has 2.7 votes which probably could not be reduced much further.

In the preprocessing the segmentation is the most time consuming part. Unfortunately region growing is not an algorithm which can easily be parallelized. Our implementation uses parallelization but that comes at the cost that we have to deal with the fact that sometimes the same segment is generated multiple times in different threads. Such cases are detected but it still means that parts of the region growing are unnecessarily done multiple times.

5. CONCLUSION AND FUTURE WORK

We have demonstrated that it is possible to detect persons in the 3D point clouds acquired by a MLS system. Our approach achieves a good runtime and consists of a preprocessing and a detection step which uses implicit shape models. We have performed an initial evaluation of the approach on a dataset which was taken in an urban environment. In this evaluation we experimented with different parameters of the approach and have analyzed their influence on the runtime and the detection performance. For this we have determined precision and recall of the different configurations. As part of an in-depth analysis of the runtime, we used a configuration which offers a good compromise between the runtime and detection performance. With this configuration we achieved a runtime of $370\,\mathrm{ms}$, a precision of 0.68 and a recall of 0.76.

In future works we plan to perform a more comprehensive evaluation of our approach which includes the usage of benchmark datasets. We plan to increase the performance of our approach with various measures. One will be to increase the amount of positive and negative training datasets. We assume this will increase the overall precision and recall of the approach. Right now the amount of used training datasets is very low which probably causes some problems in the area of generalization. We also plan to evaluate different parameterizations of the spin image descriptor which we currently use and to evaluate additional feature descriptors.

Another task will be the in depth evaluation of our preprocessing. As part of this we like to evaluate the removal of the segmentation and the subsequent filtering step to work with the unsegmented point clouds. This will solve problems with under- or over-segmentation of the data and saves the time which is needed for the segmentation. Of course it will also increase the time needed for the actual detection. To add a tracking component to our approach which should help us to increase the performance in both runtime and quality by keeping track of already detected persons and to work with multiple sensors at once are also planned for the future.

References

Behley, J., Steinhage, V. and Cremers, A. B., 2013. Laser-based segment classification using a mixture of bag-of-words. In: *2013 IEEE/RSJ International Conference on Intelligent Robots and Systems*, pp. 4195–4200.

Johnson, A. E. and Hebert, M., 1999. Using spin images for efficient object recognition in cluttered 3d scenes. *IEEE Transactions on Pattern Analysis and Machine Intelligence* 21(5), pp. 433–449.

Jüngling, K. and Arens, M., 2011. View-invariant person reidentification with an implicit shape model. In: *2011 8th IEEE International Conference on Advanced Video and Signal Based Surveillance (AVSS)*, pp. 197–202.

Knopp, J., Prasad, M., Willems, G., Timofte, R. and Van Gool, L., 2010. Hough transform and 3d surf for robust three dimensional classification. In: *Proceedings of the 11th European Conference on Computer Vision: Part VI*, ECCV'10, Springer-Verlag, Berlin, Heidelberg, pp. 589–602.

Leibe, B., Leonardis, A. and Schiele, B., 2008. Robust object detection with interleaved categorization and segmentation. *International Journal of Computer Vision* 77(1), pp. 259–289.

Maturana, D. and Scherer, S., 2015. Voxnet: A 3d convolutional neural network for real-time object recognition. In: *2015 IEEE/RSJ International Conference on Intelligent Robots and Systems (IROS)*, pp. 922–928.

Muja, M. and Lowe, D. G., 2009. Fast approximate nearest neighbors with automatic algorithm configuration. In: *International Conference on Computer Vision Theory and Application VISSAPP'09)*, INSTICC Press, pp. 331–340.

Navarro-Serment, L. E., Mertz, C. and Hebert, M., 2010. Pedestrian detection and tracking using three-dimensional ladar data. *The International Journal of Robotics Research* 29(12), pp. 1516–1528.

Premebida, C., Carreira, J., Batista, J. and Nunes, U., 2014. Pedestrian detection combining rgb and dense lidar data. In: *2014 IEEE/RSJ International Conference on Intelligent Robots and Systems*, pp. 4112–4117.

Shotton, J., Fitzgibbon, A., Cook, M., Sharp, T., Finocchio, M., Moore, R., Kipman, A. and Blake, A., 2011. Real-time human pose recognition in parts from a single depth image. In: *CVPR*, IEEE.

Shotton, J., Girshick, R., Fitzgibbon, A., Sharp, T., Cook, M., Finocchio, M., Moore, R., Kohli, P., Criminisi, A., Kipman, A. and Blake, A., 2013. Efficient human pose estimation from single depth images. *IEEE Transactions on Pattern Analysis and Machine Intelligence* 35(12), pp. 2821–2840.

Socher, R., Huval, B., Bath, B., Manning, C. D. and Ng, A. Y., 2012. Convolutional-recursive deep learning for 3d object classification. In: *Advances in Neural Information Processing Systems*, pp. 656–664.

Spinello, L., Arras, K. O., Triebel, R. and Siegwart, R., 2010. A layered approach to people detection in 3d range data. In: *AAAI*, Citeseer.

Velizhev, A., Shapovalov, R. and Schindler, K., 2012. Implicit shape models for object detection in 3d point clouds. *ISPRS Annals of Photogrammetry, Remote Sensing and Spatial Information Sciences* I-3, pp. 179–184.